



Little change in Palmer Drought Severity Index across global land under warming in climate projections

Yuting Yang^{1,7}, Shulei Zhang^{1,2,7}, Michael L. Roderick^{3,4}, Tim R. McVicar^{4,5}, Dawen Yang¹, Wenbin Liu⁶, Xiaoyan Li²

5 ¹State Key Laboratory of Hydrosience and Engineering, Department of Hydraulic Engineering, Tsinghua University, Beijing, China

²State Key Laboratory of Earth Surface Process and Resource Ecology, School of Natural Resources, Faculty of Geographical Science, Beijing Normal University, Beijing, China

³Research School of Earth Sciences, Australian National University, Canberra, ACT, Australia

10 ⁴Australian Research Council Centre of Excellence for Climate Extremes, Canberra, ACT, Australia

⁵CSIRO Land and Water, Canberra, ACT, Australia

⁶Key Laboratory of Water Cycle and Related Land Surface Processes, Institute of Geographic Sciences and Natural Resources Research, Chinese Academy of Sciences, Beijing, China

⁷Equal contribution.

15 *Correspondence to:* Yuting Yang (yuting_yang@tsinghua.edu.cn)



Abstract. Anthropogenic warming is reported to increase global drought for the 21st century when calculated using offline drought indices. However, this contradicts observations of greening and little systematic change in runoff over the past few decades and climate projections of future greening with slight increases in global runoff for the coming century. This calls into question the drought projections based on offline drought indices. To resolve this paradox, here we calculate a widely-used conventional drought index (i.e., the Palmer Drought Severity Index, PDSI) using direct outputs from 16 CMIP5 models (PDSI_CMIP5) such that the hydrologic consistency between PDSI_CMIP5 and CMIP5 models is maintained. Results show that the global PDSI_CMIP5 remains generally unchanged as climate warms, demonstrating that CMIP5 models do not actually project a general increase in PDSI drought (more reflecting soil moisture/agricultural drought) under future warming. Further analyses indicate that the projected increase in PDSI drought reported previously is primarily due to ignoring the vegetation response to elevated atmospheric CO₂ concentration ([CO₂]) in the offline calculations. On one hand, elevated [CO₂] directly reduces stomatal opening; on the other hand, elevated [CO₂] increases air temperature and thus vapor pressure deficit, which also causes partial stomatal closure. Finally, we show that the overestimation of PDSI drought can be avoided by directly using the relevant climate model outputs or by accounting for the effect of CO₂ on evapotranspiration. Our findings refute the common “warming leads to drying” perception and highlight the importance of elevated CO₂ in controlling future terrestrial hydrologic changes through vegetation responses.

1 Introduction

Drought is an intermittent disturbance of the water cycle that has profound impacts on regional water resources, agriculture and other ecosystem services (Sherwood and Fu, 2014). By taking meteorological outputs from climate model projections as the inputs to offline drought indices/hydrological impact models, numerous studies have projected increases in future drought, in terms of both frequency and severity, mainly as a consequence of warming associated with anthropogenic climate change (Cook et al., 2014, 2015; Dai, 2011, 2012; Dai et al., 2018; Huang et al., 2015, 2017; Lehner et al., 2017; Liu et al., 2018; Naumann et al., 2018; Park et al., 2018; Samaniego et al., 2018; Sternberg, 2011; Trenberth et al., 2013). The scientific basis underpinning this drying trend projected using offline drought



indices/hydrological impact models is that the calculated increases in evapotranspiration (E) are larger than the projected increase in precipitation (P) in many places (Sternberg et al., 2011), which results in
50 an increasing water deficit and thus increasing future drought. However, direct climate model outputs of
 E exhibit a much smaller increasing trend (Supplementary Figure S1) and the global land mean P is
actually projected to increase faster than its E counterpart (Greve et al., 2017; Milly and Dunne, 2016,
2017; Roderick et al., 2015; Yang et al., 2018) leading to very different conclusions.

Several recent studies have demonstrated that the drying bias in the offline calculated E trend is
55 primarily due to neglecting the impact of increasing atmospheric CO_2 concentration ($[\text{CO}_2]$) on the
water use efficiency of vegetation (Lemordant et al., 2018; Milly and Dunne, 2016, 2017; Roderick et
al., 2015; Swann et al., 2016; Yang et al., 2019). In existing hydrologic impact models/drought indices,
 P and potential evapotranspiration (E_P ; the rate of evapotranspiration that would occur with an
unlimited supply of water) are the two key input variables, which respectively represent water supply to,
60 and water demand from, the land surface. While P is a direct climate model output, E_P is neither used
nor produced by climate models. The commonly adopted procedure is to calculate E_P using the
meteorological variables contained in the climate model output using an intermediate E_P model. The
calculated E_P , together with the climate model projected P , are used to force an independent hydrologic
impact model (or hydrologic calculations embedded in drought indices) that independently calculates E ,
65 runoff (Q), and storage change (ΔS), for assessing hydrologic changes under future climate scenarios
(see Figure 1). Among various E_P models, the open-water-Penman model (Shuttleworth, 1993) and the
reference crop Penman-Monteith model (Allen et al., 1998) have been most widely used in existing
drought assessment studies, given their sound physical basis and relatively simple formulations.
Nevertheless, both Penman-based models do not faithfully capture the biological processes embedded in
70 the climate models. The open-water-Penman model was designed for water surfaces, where surface
resistance (r_s) is, by definition, equal to zero. The reference crop Penman-Monteith model assumes a
constant r_s at 70 s m^{-1} , which is appropriate for an idealized reference crop in the current climate but
contradicts the fact that r_s increases with elevated $[\text{CO}_2]$ over vegetated surfaces in climate model
projections (Yang et al., 2019). As a result, existing offline hydrologic impact models/drought indices
75 calculate estimates of E , Q and ΔS that are different from those same variables in the original fully-



coupled climate model output. For that reason, the consequent assessments of drought changes in existing offline hydrologic impact models/drought indices do not correctly represent the projections in the underlying fully-coupled climate models. Figure 1 illustrates the inconsistency in the hydrologic predictions (also see Milly and Dunne 2017) that have resulted in different trends in projected future
80 drought between climate models and offline hydrologic impact models/drought indices.

Here, we re-assess changes in future global drought using climate model projections from 16 Coupled-Model-Intercomparison-Project-Phase-5 (CMIP5) models under historical (1861-2005) and Representative Concentration Pathway 8.5 (RCP8.5; 2006-2100) experiments (Taylor et al., 2012). The Palmer Drought Severity Index (PDSI; Palmer, 1965) is adopted here to quantify drought as it has been
85 widely used for operational drought monitoring and is increasingly used in studies assessing drought under climate change (Cook et al., 2014, 2015; Dai, 2011, 2012; Dai et al., 2018; Lehner et al., 2017; Liu et al., 2018; Sheffield et al., 2012; Swann et al., 2016; Trenberth et al., 2013). To maintain consistency between the calculated PDSI and the CMIP5 models, we calculate PDSI using direct hydrologic outputs (i.e., P , E , Q , ΔS) from the CMIP5 models (PDSI_CMIP5; see Methods). This
90 procedure minimizes the uncertainty in PDSI estimates caused by uncertainties in the hydrologic simulations embedded in the original PDSI algorithm (Palmer, 1965). The original PDSI using reference crop Penman-Monteith E_P (PDSI_PM-RC), as extensively used previously (e.g., Cook et al., 2014, 2015; Liu et al., 2018), and is also presented for comparison (the right stream shown in Figure 1). Additionally, to demonstrate the impact of elevated $[\text{CO}_2]$ on PDSI via vegetation feedbacks, we
95 calculate PDSI forced with E_P estimated from a modified Penman-Monteith equation that explicitly considers the biological effect of elevated $[\text{CO}_2]$ (the left stream in Figure 1) on r_s (PDSI_PM $[\text{CO}_2]$; see Methods).

2 Data and Methods

2.1 Climate model projections

100 We used outputs from 16 climate models participating in Phase 5 of the Coupled Model Intercomparison Project (CMIP5; Supplementary Table S1) under historical (1861-2005) and RCP 8.5



(2006-2100) experiments (Taylor et al., 2012). We used monthly series of runoff, precipitation, soil moisture, sensible and latent heat flux at the land surface along with near-surface air temperature, air pressure, wind speed and specific humidity. All outputs from 16 CMIP5 models were resampled to a
105 common 1° spatial resolution by using the first-order conservative remapping scheme (Jones, 1999).

2.2 Calculation of PDSI

The Palmer Drought Severity Index (PDSI) was used to quantify drought (Palmer, 1965). To minimize the impact of initial conditions on PDSI estimates, the first 40 years (1861-1900) are used for model spin-up with the analyses focused on the 1901-2100 period. Briefly, the PDSI model consists of two
110 parts: (i) a two-stage bucket model that calculates the monthly water balance components (i.e., actual evapotranspiration (E), runoff (Q) and soil moisture changes (ΔS)) using P and E_P as inputs, and (ii) a dimensionless index that describes the moisture departure between the actual precipitation and the precipitation needed to maintain a normal soil moisture level for a given time (i.e., the climatically appropriate for existing conditions values). Detailed descriptions of PDSI can be found in Palmer
115 (1965). A drought event is identified with negative PDSI values, with a more negative PDSI indicating a more severe drought, whereas moist events are associated with positive PDSI values.

We calculated PDSI following Palmer (1965) yet calculated E_P using the reference crop Penman-Monteith model (PDSI_PM-RC). The Penman-Monteith model explicitly considers influences from both radiative and aerodynamic components and has been widely used in previous PDSI calculations
120 (e.g., van der Schrier et al., 2011; Dai et al., 2011; Sheffield et al., 2012). In addition, we also used a modified Penman-Monteith model (PM[CO₂]; detailed later in the Methods and also see Yang et al., 2019) that accounts for the impact of elevated [CO₂] on r_s to calculate E_P and then PDSI (PDSI_PM[CO₂]). Applying this modified Penman-Monteith model with [CO₂] adjustment in a simple hydrologic model satisfactorily recovered the hydrologic predictions of CMIP5 models (Yang et al.,
125 2019).

Additionally, instead of using hydrological simulations from the simplified water balance model embedded in the original PDSI model, we also calculated PDSI by using direct hydrologic outputs E , Q ,



ΔS from the 16 CMIP5 models (PDSI_CMIP5). This approach ensures that PDSI_CMIP5 faithfully represented the CMIP5 output. As the original PDSI model depends on a two-stage “bucket” model of the soil, we correspondingly regarded the moisture in upper portion of soil column (integrated over the uppermost 10 cm) from CMIP5 models as the moisture in the first layer and the total soil moisture content as the available moisture in both layers. Moreover, since the estimation of the weighting factor that converts moisture anomalies into the PDSI index also requires knowledge of E_P , we used the E_P computed from a modified Penman-Monteith equation that explicitly considers the biological effect of elevated $[\text{CO}_2]$ (i.e., $\text{PM}[\text{CO}_2]$) (Yang et al., 2019). To further assist understanding how different PDSIs were calculated, we illustrate the calculation procedures of different PDSIs in Figure 2. Additionally, Matlab codes with worked examples of the different PDSIs can be accessed through <https://github.com/zslthu/Calculate-PDSI-in-Matlab>. The PDSIs were calculated using outputs of each CMIP5 model in turn, and the ensemble PDSIs (averaging PDSIs over models) were used in the following analyses.

2.3 Calculation of Potential Evapotranspiration

Two potential evapotranspiration formulations were used to calculate E_P . The first is the reference crop Penman-Monteith E_P model, which computes E_P (mm day^{-1}) as (Allen et al., 1998):

$$E_P = \frac{0.408\Delta R_n^* + \gamma \frac{900}{T + 273} uD}{\Delta + \gamma(1 + 0.34u)} \quad (1)$$

where Δ (Pa K^{-1}) is the gradient of the saturation vapour pressure with respect to temperature, γ (Pa K^{-1}) is the psychrometric constant, R_n^* ($\text{MJ m}^{-2} \text{day}^{-1}$) is the surface available radiation (i.e., net radiation minus ground heat flux), D (Pa) is the vapour pressure deficit of the air at 2 m height, u (m s^{-1}) is the wind speed at 2 m height. In the reference crop Penman-Monteith model, r_s is set to a fixed value of 70 s m^{-1} and this parameter value is embedded into the equation.



150 In addition, we used a modified reference crop Penman-Monteith E_P model (i.e., PM[CO₂]) that accounts for the impact of rising [CO₂] (expressed in ppm units) on r_s , as derived in Yang et al. (2019). The PM[CO₂] model calculates E_P as:

$$E_P = \frac{0.408\Delta R_n^* + \gamma \frac{900}{T + 273} uD}{\Delta + \gamma \{1 + u[0.34 + 2.4 \times 10^{-4} ([CO_2] - 300)]\}} \quad (2)$$

2.4 Determining the timing of global warming target

155 To demonstrate the impact of warming on drought changes, we assessed changes in PDSI_CMIP5 under two future warming targets: 1.5 °C and 2 °C warming above the pre-industrial level. The 1.5 °C and 2 °C warming levels have been extensively discussed (Huang et al., 2017; Lehner et al., 2017; Liu et al., 2018; Park et al., 2018; Samaniego et al., 2018), as they are the two key warming targets set in the Paris Agreement on climate change (UNFCCC, 2015). The timing when the global warming targets (i.e.,
160 $t_{1.5}$ and t_2) is reached in each of the 16 CMIP5 models was computed based on the model output of the near-surface air temperature (T_a). We first selected 1986–2005 as the baseline period, which is a widely used reference period for climate impact assessment (Lehner et al., 2017; Liu et al., 2018; Park et al., 2018). Then, we applied a 20-year moving average filter to the global mean annual T_a time series to remove the interannual fluctuations in annual T_a (Liu et al., 2018; Park et al., 2018). Each 20-year
165 moving average is indexed to its final year (for example, the 20-year running mean T_a for 2080 is an average of T_a for 2061–2080). Finally, $t_{1.5}$ and t_2 are respectively determined at the times when global mean T_a reached 0.9 °C and 1.4 °C above the 1986–2005 baseline, as this period was at least 0.6 °C warmer than the pre-industrial level (Hawkins et al., 2017; Schleussner et al., 2016).

3 Results

170 3.1 Predicted drought changes

In applications, a PDSI < -3.0 is considered to be drought conditions while a PDSI > 3.0 is considered exceptionally moist (e.g., Palmer, 1965; Liu et al., 2018). We examined changes in the land area subject



to these dry and moist extremes and find that the global drought area (i.e., $PDSI < -3.0$) during the 21st century increases by $0.2393 \pm 0.0942\%$ per year ($p < 0.01$) for $PDSI_{PM-RC}$ but only increases by
175 $0.1099 \pm 0.0228\%$ per year ($p < 0.01$) for $PDSI_{CMIP5}$ and $0.1178 \pm 0.0308\%$ per year ($p < 0.01$) for
 $PDSI_{PM[CO_2]}$, respectively (Figures 3a-c). Evident drought increases are depicted by $PDSI_{PM-RC}$
across much of the North America, South America, central-to-south Europe, Congo Basin, southern
Africa, southeast China and southern coastal areas of Australia (Figure 3e), as widely reported
previously (Dai, 2011, 2012; Dai et al., 2018; Cook et al., 2014; Lehner et al., 2018; Liu et al., 2018).
180 However, that trend is not identified by $PDSI_{CMIP5}$ and $PDSI_{PM[CO_2]}$ (Figures 3e and f). By
contrast, moist areas (i.e., $PDSI > 3.0$) are less divergent among the three PDSIs, although the
 $PDSI_{PM-RC}$ still shows the fewest wetting lands compared to the other two PDSIs. Interestingly, both
 $PDSI_{CMIP5}$ and $PDSI_{PM[CO_2]}$ depict the increase in drought area to be more or less the same as the
increase in moist area (Figures 3a-c). A similar result that the increase in drought area is essentially the
185 same as the increase in moist area is obtained when the PDSI thresholds are changed to $PDSI < -2.0$ and
 $PDSI > 2.0$ (Supplementary Figure S2).

The above results clearly indicate an inconsistency between the $PDSI_{PM-RC}$ that has been widely
used in offline calculations for drought assessment studies and the underlying CMIP5 models, as the
 $PDSI_{CMIP5}$ used here is based on the direct hydrologic outputs (E , Q and ΔS) from CMIP5 models.
190 To give a global overview, we compare the time series of the three global average PDSI in Figure 4.
Not surprisingly, the three global average PDSI time series exhibit remarkably different trends since the
year 2000, with $PDSI_{PM-RC}$ showing a significant decreasing trend ($-0.0130 \pm 0.0059 \text{ yr}^{-1}$; $p < 0.01$)
but $PDSI_{CMIP5}$ remains more or less unchanged over the entire period ($0.0004 \pm 0.0015 \text{ yr}^{-1}$; not
significant) (Figure 3). In comparison, the global average time series of $PDSI_{PM[CO_2]}$ (trend = -
195 $0.0002 \pm 0.0024 \text{ yr}^{-1}$; not significant) closely follows that of $PDSI_{CMIP5}$ for the entire study period
(Figure 3), highlighting the importance of vegetation response to elevated $[CO_2]$ in the control of future
surface hydrological changes. This latter comparison further confirms that the inconsistency between
the $PDSI_{PM-RC}$ and CMIP5 models is largely caused by ignoring the vegetation response to elevated
 $[CO_2]$ in the $PDSI_{PM-RC}$. A similar result that $PDSI_{PM-RC}$ shows a significant decreasing trend
200 while $PDSI_{CMIP5}$ and $PDSI_{PM[CO_2]}$ remain more or less unchanged is obtained when considering



the entire globe as one point, that is, averaging the forcing variables first and then do the PDSI calculation (Supplementary Figure S3).

3.2 The effect of warming on drought changes

Warming has been identified as the key driver of the overall future drought increase in numerous studies (Cook et al., 2014, 2015; Dai, 2011, 2012; Dai et al., 2018; Huang et al., 2015, 2017; Lehner et al., 2017; Liu et al., 2018). To further understand the impact of warming on drought changes, we assessed changes in PDSI_CMIP5 at 1.5 °C and 2 °C warming above the pre-industrial level. The PDSI_PM-RC is also presented for comparison. Any substantial increase in drought is identified when PDSI for a future warming target decreased by 1.0 compared to PDSI during the 1986-2005 baseline (i.e., $\Delta\text{PDSI} < -1$). Additionally, only places where the $\Delta\text{PDSI} < -1.0$ threshold is reached in at least 8 CMIP5 model (out of the 16 CMIP5 models 50% and more) are considered to be robust projections and thus used herein. Based on the PDSI_CMIP5, our results show that almost nowhere on earth (only 0.06% of the global land area) is projected to have a substantial drought increase at the 1.5 °C warming target, and this number only slightly increases to 0.77% at the 2 °C warming target (Figures 5a and b). In comparison, substantial increase in drought is identified at 5.10 % and 13.41 % of the global land area at the two warming targets, respectively, when PDSI_PM-RC is used (Figures 5a and c). More places are projected to have a substantial drought increase under future warming if we relaxed the threshold of PDSI change to -0.5 (i.e., $\Delta\text{PDSI} < -0.5$) (Figure 5d-f). Nevertheless, the PDSI_CMIP5 still shows a considerable smaller percentage of drying lands (6.2% and 10.0%) than the PDSI_PM-RC (26.32% and 34.77%) under the two warming targets, respectively, particularly over North America, much of Amazonia, Europe, the Congo basin and southeast China.

4 Discussion and concluding remarks

The above results clearly demonstrate an overestimation of drought severity and extent using PDSI in many previous assessments of future drought (e.g., Cook et al., 2014, 2015; Dai, 2011, 2012; Dai et al., 2018; Lehner et al., 2018; Liu et al., 2018). The overestimation is primarily caused by neglecting the impact of elevated $[\text{CO}_2]$ on r_s and consequently on E_P in the offline calculation of drought indices. As



E_P is neither used nor produced by climate models, an offline intermediate E_P model is required to estimate E_P based on climate outputs of meteorological variables. However, conventional E_P models, such as the open-water Penman model and the reference crop Penman-Monteith model, involve an important assumption that r_s remains constant over time (Allen et al., 1998; Shuttleworth, 1993). This assumption is in general valid for water surfaces and/or wet bare soils but proved to be problematic over vegetated surfaces. Over vegetated surfaces, on one hand, elevated $[\text{CO}_2]$ leads to a partial stomatal closure that increase r_s (e.g., Ainsworth and Rogers, 2007) yet on the other hand, elevated $[\text{CO}_2]$ has “fertilized” vegetation resulting in an increased foliage cover (e.g., Donohue et al., 2013; Zhu et al., 2016), which also effectively suggests a reduction in r_s . In addition, elevated $[\text{CO}_2]$ serves as the ultimate driver of climate warming in the CMIP5 models and consequently leads to an increase in atmospheric vapor pressure deficit, which also tends to increase r_s (Lin et al., 2018; Novick et al., 2016).

While the net effect of elevated $[\text{CO}_2]$ on r_s is still uncertain in the real world, our results clearly indicate that in CMIP5 models, elevated $[\text{CO}_2]$ increases r_s , which, with all else equal, results in a decrease of E_P and thus E . A recent study further showed that over vegetated surfaces, an increase in E_P caused by warming-induced vapor pressure deficit increase is almost entirely offset by a decrease in E_P caused by the increase in r_s driven by elevated $[\text{CO}_2]$ in CMIP5 models (Yang et al., 2019). This suggests that warming does not necessarily lead to a higher E_P over vegetated surfaces and hence increased drought under $[\text{CO}_2]$ enrichment, which is consistent with CMIP5 model projections yet contradicts the perception that “warming leads to drying” in many previous studies (Cook et al., 2014, 2015; Dai, 2011, 2012; Dai et al., 2018; Huang et al., 2015, 2017; Lehner et al., 2018; Liu et al., 2018; Park et al., 2018; Samaniego et al., 2018; Sternberg, 2011; Trenberth et al., 2013). Additionally, it is worthwhile mentioning that the CMIP5 models do project topsoil moisture (within 10 cm) to decline similar to PDSI_PM-RC (Dai, 2012; Dai et al., 2018), but that since no systematic decline in runoff or in vegetation indicators (e.g., leaf area index and gross/net primary production) seems to result from it (Greve et al., 2017; Milly and Dunne, 2016, 2017; Roderick et al., 2015; Swann et al., 2016; Yang et al., 2019), it does not seem to actually matter. This is likely because root-zone or deeper soil moisture that is of more agricultural/ecological and/or hydrological significance, is projected to remain more or less

unchanged (Berg et al., 2017; Greve et al., 2017), consistent with PDSI_CMIP5 and PDSI_PM[CO₂]
255 (Figures 3 and 4).

Here, we use PDSI as an illustrating case; similar results were also found in another commonly used
drought index (i.e., the Standardized Precipitation-Evapotranspiration Index, or SPEI; Vicente-Serrano,
2010) (Supplementary Figure S4). Nevertheless, both PDSI and SPEI, as well as other drought/aridity
metrics, are secondary offline impact models. Since climate models are fully-coupled land (and ocean)
260 – atmosphere models that are an internally consistent representation of the climate system (Milly and
Dunne, 2016), a scientific prior of applying any offline hydrological impact models is that the adopted
model must be able to recover the hydrological simulations in climate models (Roderick et al., 2015;
Milly and Dunne, 2017; Yang et al., 2019). Otherwise, any inconsistency in hydrological predictions
between offline impact models and climate models themselves would lead to inconsistent predictions in
265 other components of the climate system. Unfortunately, this important scientific prior has been largely
ignored in many previous drought assessment studies, leading to biased drought predictions that are
actually inconsistent with climate model themselves.

In summary, we have shown that climate model projections of the global drought area remains more or
less constant over a 200-year period under different scenarios for future warming. Our results
270 demonstrate that the “warming leads to drying” perception is fundamentally flawed, primarily due to the
ignorance of the vegetation response to elevated [CO₂] (also see Yang et al., 2019). However, despite a
small overall trend globally, we find that both drying and wetting areas are simulated to increase
towards the end of this century (Figures 3b-f), suggesting an increased spatial variability in surface
hydrological conditions that will likely lead to increased droughts and/or floods at local/regional scales.
275 In this light, attention should be paid to regions where droughts and/or floods are projected to most
likely increase (e.g., Mediterranean Europe and Central America) and more efforts may be needed to
mitigate the consequent impact there under climate change.



Code availability

Matlab codes with worked examples of the different PDSIs can be accessed through
280 <https://github.com/zslthu/Calculate-PDSI-in-Matlab>

Data availability

The data that support the findings of this study are openly available (<http://cmip-pcmdi.llnl.gov/cmip5/>).

Author contribution

Y. Yang and M. Roderick designed the study. S. Zhang and Y. Yang performed the calculation and
285 drafted the manuscript. All authors contributed to results discussion and manuscript writing;

Competing interests

The authors declare that they have no conflict of interest

Acknowledgements

This study was supported by the National Natural Science Foundation of China (Grant No. 41890821)
290 and the Qinghai Department of Science and Technology (Grant No. 2019-SF-A4). M. Roderick
acknowledges the support of the Australian Research Council (CE170100023). T. McVicar
acknowledges support from CSIRO Land and Water.

References

Allen, R. G., Pereira, L. S., Raes, D., and Smith, M.: Crop Evapotranspiration-guidelines for Computing
295 Crop Water Requirements, FAQ Irrigation and Drainage Paper 56, FAO, Rome, 300 pp, 1998.

Ainsworth, A. E., and Rogers, A.: The response of photosynthesis and stomatal conductance to rising
[CO₂]: mechanisms and environmental interactions, *Plant Cell Environ.*, 30, 258-270,
<https://doi.org/10.1111/j.1365-3040.2007.01641.x>, 2007.



- 300 Berg, A., Sheffield, J., and Milly, P. C. D.: Divergent surface and total soil moisture projections under
global warming, *Geophys. Res. Lett.*, 44, 236-244, <https://doi.org/10.1002/2016GL071921>, 2017.
- Cook, B. I., Smerdon, J. E., Seager, R., and Coats, S.: Global warming and 21st century drying, *Clim.
Dyn.*, 43, 2607-2627, <https://doi.org/10.1007/s00382-014-2075-y>, 2014.
- Cook, B. I., Ault, T. R. and Smerdon, J. E.: Unprecedented 21st century drought risk in the American
Southwest and Central Plains Science, *Advances*, 1, e1400082, <https://doi.org/10.1126/sciadv.1400082>,
305 2015.
- Dai, A.: Drought under global warming: a review, *Wiley Interdiscip. Rev. Clim. Change*, 2, 45-65,
<https://doi.org/10.1002/wcc.81>, 2011.
- Dai, A.: Increasing drought under global warming in observations and models, *Nat. Clim. Change*, 3, 52,
<https://doi.org/10.1038/nclimate1633>, 2012.
- 310 Dai, A., Zhao, T., and Chen, J.: Climate Change and Drought: a Precipitation and Evaporation
Perspective, *Current Clim. Change Reports*, 4, 301-312, <https://doi.org/10.1007/s40641-018-0101-6>,
2018.
- Donohue, R. J., Roderick, M. L., McVicar, T. R., and Farquhar, G. D.: Impact of CO₂ fertilization on
maximum foliage cover across the globe's warm, arid environments, *Geophys. Res. Lett.*, 40, 3031-
315 3035, <https://doi.org/10.1002/grl.50563>, 2013.
- Greve, P., Roderick, L. R., and Seneviratne, S. I.: Simulated changes in aridity from the last glacial
maximum to 4xCO₂, *Environ. Res. Lett.*, 12, 114021, <https://doi.org/10.1088/1748-9326/aa89a3>, 2017.
- Hawkins, E., Ortega, P., Suckling, E., Schurer, A., Hegerl, G., Jones, P., Joshi, M., Osborn, T. J.,
Masson-Delmotte, V., Mignot, J., Thorne, P., and van Oldenborgh, G. J.: Estimating Changes in Global
320 Temperature since the Preindustrial Period, *Bull. Am. Meteorol. Soc.*, 98, 1841-1856,
<https://doi.org/10.1175/BAMS-D-16-0007.1>, 2017.
- Huang, J., Yu, H., Guan, X., Wang, G., and Guo, R.: Accelerated dryland expansion under climate
change, *Nat. Clim. Change*, 6, 166-171, <https://doi.org/10.1038/nclimate2837>, 2016.
- Huang, J., Yu, H., Dai, A., Wei, Y., and Kang, L.: Drylands face potential threat under 2 °C global
325 warming target, *Nat. Clim. Change*, 7, 417-422, <https://doi.org/10.1038/nclimate3275>, 2017.



- Jones, P. W.: First- and Second-Order Conservative Remapping Schemes for Grids in Spherical Coordinates, *Mon. Weather Rev.*, 127, 2204-2210, [https://doi.org/10.1175/1520-0493\(1999\)127<2204:FASOCR>2.0.CO;2](https://doi.org/10.1175/1520-0493(1999)127<2204:FASOCR>2.0.CO;2), 1999.
- 330 Lehner, F., Coats, S., Stocker, T. F., Pendergrass, A. G., Sanderson, B. M., Raible, C. C., and Smerdon, J. E.: Projected drought risk in 1.5°C and 2°C warmer climates, *Geophys. Res. Lett.*, 44, 7419-7428, <https://doi.org/10.1002/2017GL074117>, 2017.
- Lemordant, L., Gentine, P., Swann, A. S., Cook, B. I., and Scheff, J.: Critical impact of vegetation physiology on the continental hydrologic cycle in response to increasing CO₂, *Proc. Natl. Acad. Sci.*, 115, 4093-4098, <https://doi.org/10.1073/pnas.1720712115>, 2018.
- 335 Lin, C., Gentine, P., Huang, Y., Guan, K., Kimm, H., and Zhou, S.: Diel ecosystem conductance response to vapor pressure deficit is suboptimal and independent of soil moisture, *Agr. Forest Meteorol.*, 15, 24-34, <https://doi.org/10.1016/j.agrformet.2017.12.078>, 2018.
- Liu, W., Sun, F., Lim, W. H., Zhang, J., Wang, H., Shiogama, H., and Zhang, Y.: Global drought and severe drought-affected populations in 1.5 and 2 °C warmer worlds, *Earth Syst. Dynam.*, 9, 267-283, 340 <https://doi.org/10.5194/esd-9-267-2018>, 2018.
- Massmann, A., Gentine, P., and Lin, C.: When does vapor pressure deficit drive or reduce evapotranspiration?, *Journal of Advances in Modelling Earth Systems*, 11, <https://doi.org/10.1029/2019MS001790>, 2019.
- Milly, P. C. D., and Dunne, K. A.: Potential evapotranspiration and continental drying, *Nat. Clim. Change*, 6, 946-949, <https://doi.org/10.1038/nclimate3046>, 2016.
- 345 Milly, P. C. D., and Dunne, K. A.: Hydrologic Drying Bias in Water-Resource Impact Analyses of Anthropogenic Climate Change, *J. Am. Water Resour. Assoc.*, 53, 822-838, <https://doi.org/10.1111/1752-1688.12538>, 2017.
- Naumann, G., Alfieri, L., Wyser, L., Mentaschi, L., Betts, R. A., Carrao, H., Spinoni, J., Vogt, J., and Feyen, L.: Global Changes in Drought Conditions under Different Levels of Warming, *Geophys. Res. Lett.*, 45, 3285-3296, <https://doi.org/10.1002/2017GL076521>, 2018.
- 350 Novick, K.A., Ficklin, D. L., Stoy, P., Williams, C. A., Bohrer, G., Oishi, A. C., Papuga, S. A., Blanken, P. D., Noormets, A., Sulman, B. N., Scott, R. L. Wang, L., Phillips, R. P.: The increasing importance of



- atmospheric demand for ecosystem water and carbon fluxes, *Nature Clim. Change*, 6, 1023-1027,
355 <https://doi.org/10.1038/nclimate3114>, 2016.
- Palmer, W. C.: Meteorological drought Research Paper No. 45, US Department of Commerce Weather Bureau, Washington, DC, USA, 58 pp, 1965.
- Park, C. -E., Jeong, S., Joshi, M., Osborn, T. J., Ho, C. H., Piao, S., Chen, D., Liu, J., Yang, H., Park, H., Kim, B. M., and Feng, S.: Keeping global warming within 1.5 °C constrains emergence of aridification,
360 *Nat. Clim. Change*, 8, 70-74, <https://doi.org/10.1038/s41558-017-0034-4>, 2018.
- Roderick, M. L., Greve, P., and Farquhar, G. D.: On the assessment of aridity with changes in atmospheric CO₂, *Water Resour Res.*, 51, 5450-5463, <https://doi.org/10.1002/2015WR017031>, 2015.
- Samaniego, L., Thober, S., Kumar, R., Wanders, N., Rakovec, O., Pan, M., Zink, M., Sheffield, J., and Wood, E. F.: Anthropogenic warming exacerbates European soil moisture droughts, *Nat. Clim. Change*,
365 8, 421-426, <https://doi.org/10.1038/s41558-018-0138-5>, 2018.
- Schleussner, C. F., Rogelj, J., Schaeffer, M., Lissner, T., Licker, R., Fischer, E. M., Knutti, R., Levermann, A., Frieler, K., and Hare, M.: Science and policy characteristics of the Paris Agreement temperature goal, *Nat. Clim. Change*, 6, 827-835, <https://doi.org/10.1038/nclimate3096>, 2016.
- Sheffield, J., Wood, E. F., and Roderick, M. L.: Little change in global drought over the past 60 years,
370 *Nature*, 491, 435-438, <https://doi.org/10.1038/nature11575>, 2012.
- Sherwood, S., and Fu, Q.: A drier future?, *Science*, 343, 73, <https://doi.org/10.1126/science.1247620>, 2014.
- Shuttleworth, W. J.: Evaporation, in *Handbook of Hydrology*, edited by: Maidment, D. R. McGraw-Hill Education, New York, USA, 98-144, 1993.
- 375 Sternberg, T.: Regional drought has a global impact, *Nature*, 472, 169, <https://doi.org/10.1038/472169d>, 2011.
- Swann, A. L. S., Hoffman, F. M., Koven, C. D., and Randerson, J. T.: Plant responses to increasing CO₂ reduce estimates of climate impacts on drought severity, *Proc. Natl. Acad. Sci.*, 113, 10019-10024, <https://doi.org/10.1073/pnas.1604581113>, 2016.
- 380 Taylor, K. E., Stouffer, R. J., and Meehl, G. A.: An Overview of CMIP5 and the Experiment Design, *Bull. Am. Meteorol. Soc.*, 93, 485-498, <https://doi.org/10.1175/BAMS-D-11-00094.1>, 2012.



- Trenberth, K. E., Dai, A., van der Schrier, G., Jones, P. D., Barichivich, J., Briffa, K. R., and Sheffield, J.: Global warming and changes in drought, *Nat. Clim. Change*, 4, 17-22, <https://doi.org/10.1038/nclimate2067>, 2014.
- 385 UNFCCC. Adoption of the Paris Agreement, Proposal by the President Report No. FCCC/CP/2015/L.9. (United Nations, 2015).
- Vicente-Serrano, S. M., Begueria, S., and Lopez-Moreno, J. I. A.: A Multiscalar Drought Index Sensitive to Global Warming: The Standardized Precipitation Evapotranspiration Index, *J. Clim.*, 23, 1696-1718, <https://doi.org/10.1175/2009JCLI2909.1>, 2010.
- 390 Yang, Y. T., Zhang, S., McVicar, T. R., Beck, H. E., Zhang, Y. Q., and Liu, B.: Disconnection between trends of atmospheric drying and continental runoff, *Water Resour. Res.*, 54, 4700-4713, <https://doi.org/10.1029/2018WR022593>, 2018.
- Yang, Y. T., Roderick, M. L., Zhang, S., McVicar, T. R., and Donohue, R. J.: Hydrologic implications of vegetation response to elevated CO₂ in climate projections, *Nat. Clim. Change*, 9, 44-48, <https://doi.org/10.1038/s41558-018-0361-0>, 2019.
- 395
- Zhu, Z., Piao, S., Myneni, R. B., Huang, M., Zeng, Z., Canadell, J. G., Ciais, P., Sitch, S., Friedlingstein, P., Arneth, A., Cao, C., Cheng, L., Kato, E., Koven, C., Li, Y., Lian, X., Liu, Y., Liu, R., Mao, J., Pan, Y., Peng, S., Peñuelas, J., Poulter, B., Pugh, T., Stocker, B. D., Viovy, N., Wang, X., Wang, Y., Xiao, Z., Yang, H., Zaehle, S., Zeng N.: Greening of the earth and its drivers, *Nat. Clim. Change*, 6, 791–795, <https://doi.org/10.1038/nclimate3004>, 2016.
- 400



List of figures

Figure 1: Conceptual plot illustrating the inconsistency in the hydrologic predictions between climate models and offline hydrologic impact models.

405 Figure 2: Flowchart of PDSI calculations.

Figure 3: Global average time series of fractional land area experiencing drought/moist conditions and the spatial pattern of PDSI trend.

Figure 4: Global average time series of the PDSI during 1901-2100.

Figure 5: Areas with substantial drought increase under future warming.

410

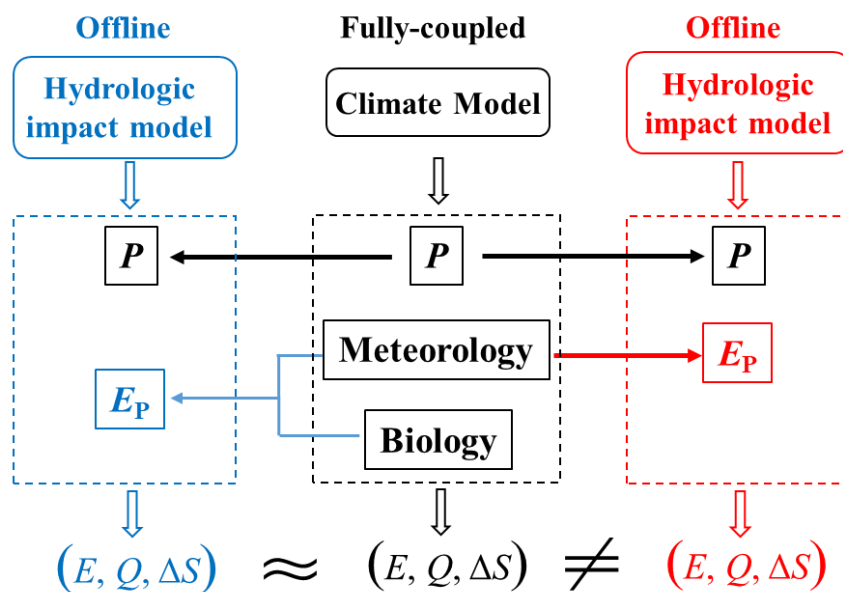
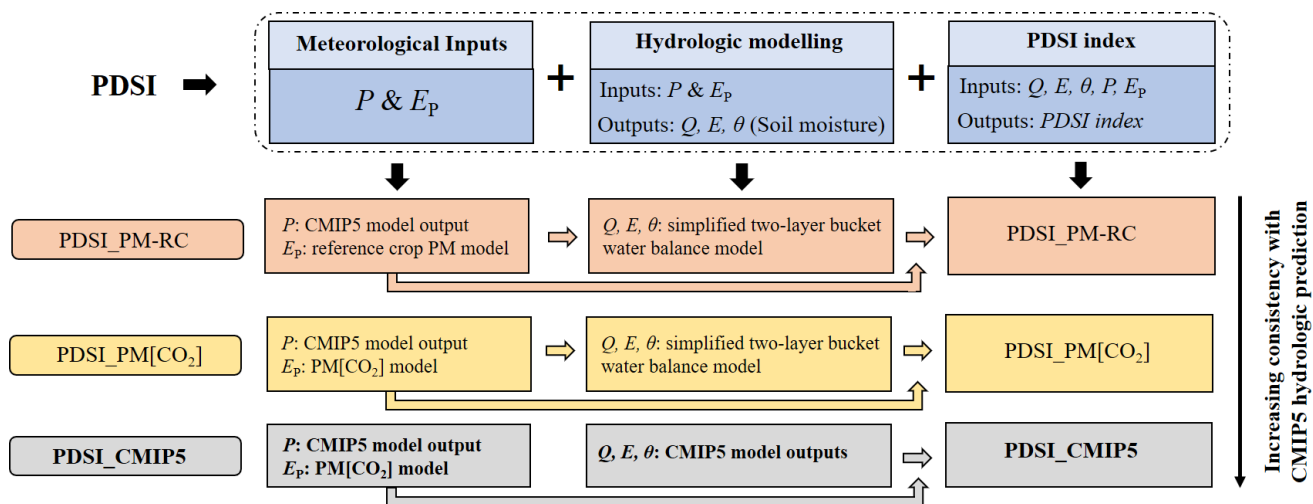


Figure 1: Conceptual plot illustrating the inconsistency in the hydrologic predictions between climate models and offline hydrologic impact models. The symbols P , E_P , E , Q and ΔS represent precipitation, potential evapotranspiration, actual evapotranspiration, runoff and storage change, respectively. The meteorological variables used to calculate E_P depend on the adopted E_P model but mainly include net radiation, near-surface air temperature, vapor pressure and wind speed. The biological factor here is the response of surface resistance to elevated $[\text{CO}_2]$ over vegetated lands.



425

Figure 2: Flowchart of PDSI calculations.

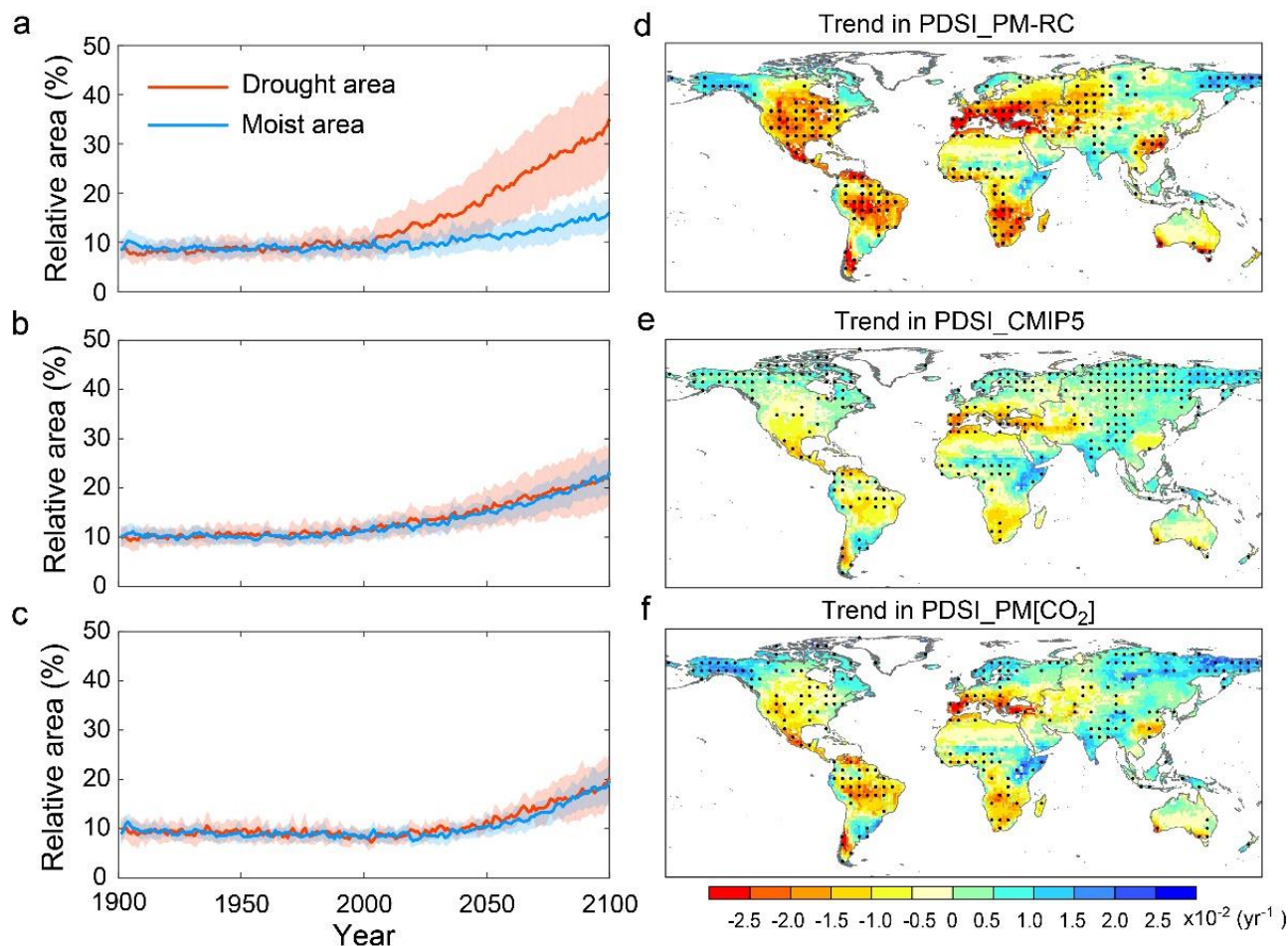


Figure 3: Global average time series of fractional land area experiencing drought/moist

430 **conditions and the spatial pattern of PDSI trend. a-c,** Global average time series of land area
experiencing drought (PDSI < -3.0, red) and moist (PDSI > 3.0, blue) conditions for (a) PDSI_PM-RC,
(b) PDSI_CMIP5 and (c) PDSI_PM[CO₂], respectively. The solid curves represent the ensemble mean
of 16 CMIP5 models and the shading represents plus/minus one standard deviation among models. **e-f,**
spatial distribution of PDSI trends during 1901-2100 for (d) PDSI_PM-RC, (e) PDSI_CMIP5 and (f)
435 PDSI_PM[CO₂], respectively. Black dots represent locations where the same sign of the PDSI trend is
identified in at least 8 out of the 16 CMIP5 models (i.e., >50 % of models).

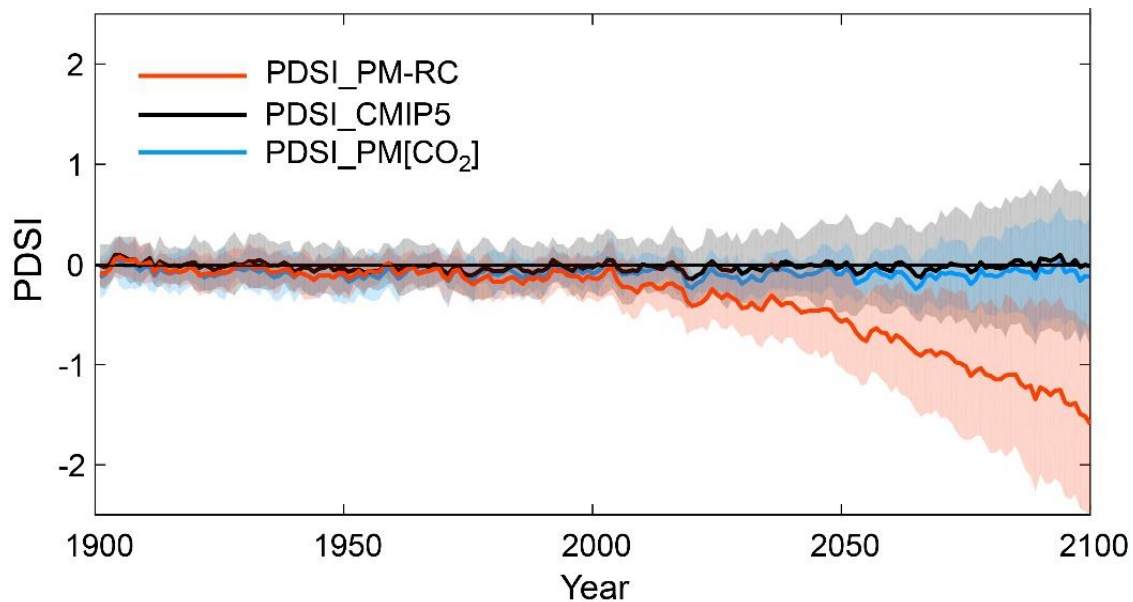


Figure 4: Global average time series of the PDSI during 1901-2100. PDSI_PM-RC (red), PDSI_CMIP5 (black) and PDSI_PM[CO₂] (blue). The solid curve represents the ensemble mean of the 16 CMIP5 models and the shading represents plus/minus one standard deviation among the 16 models. The time series are averaged over global land areas excluding Greenland and Antarctica.

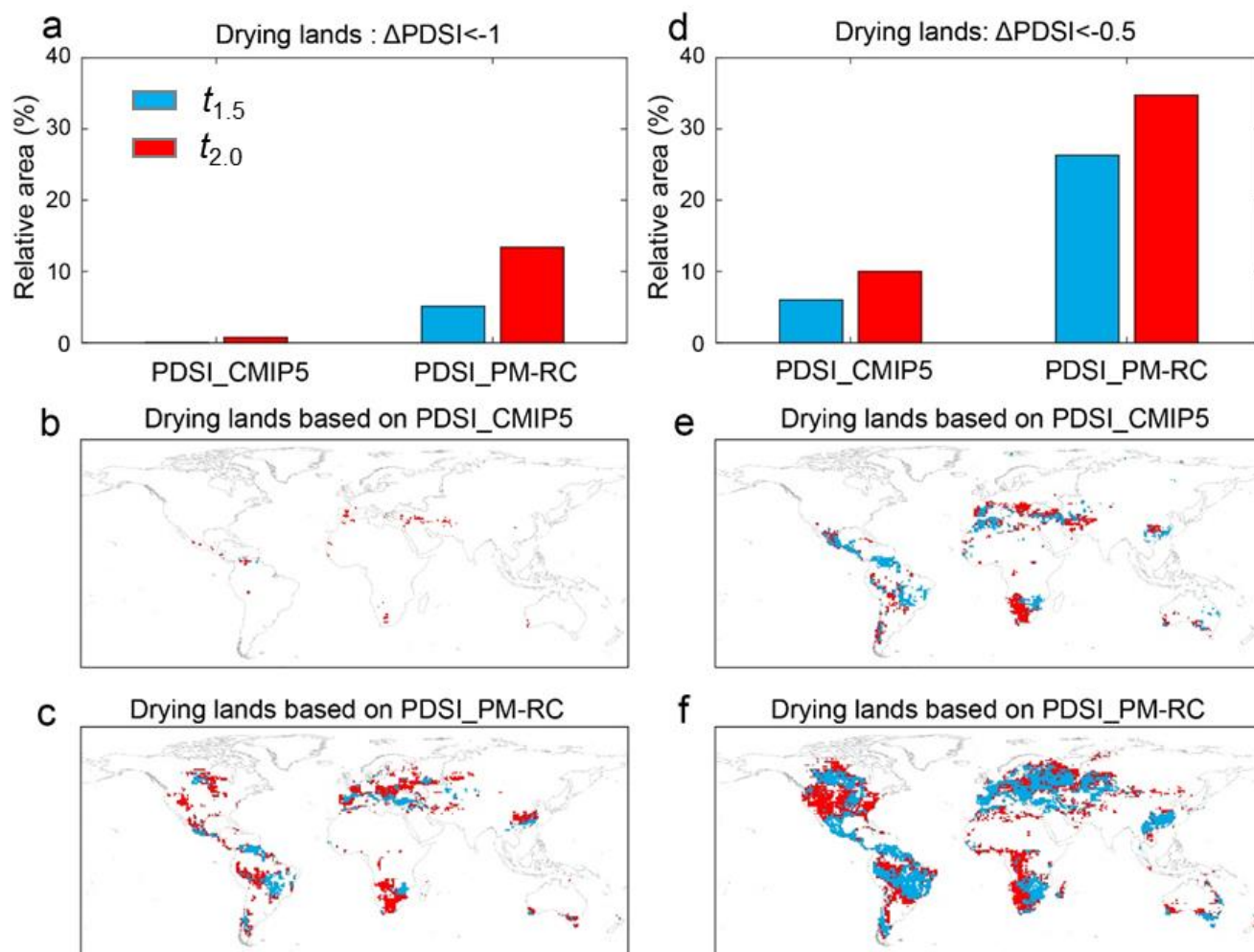


Figure 5: Areas with substantial drought increase under future warming. **a**, Relative land area with substantial drought increase ($\Delta\text{PDSI} < -1.0$) under 1.5 °C and 2 °C warming based on PDSI_CMIP5 and PDSI_PM-RC. **b-c**, Spatial pattern of substantial drought increase ($\Delta\text{PDSI} < -1.0$) under 1.5 °C and 2 °C warming based on (b) PDSI_CMIP5 and (c) PDSI_PM-RC. **d-f**, Similar with a-c but for $\Delta\text{PDSI} < -0.5$.